1-1-2003

Online Monitoring of Anode Outlet CO Concentration in PEM Fuel Cells

J. X. Zhang

Ravindra Datta
Worcester Polytechnic Institute, rdatta@wpi.edu

Electrochemical and Solid-State Letters, **6** (1) A5-A8 (2003)
0013-4651/2002/6(1)/A5/4/$7.00 © The Electrochemical Society, Inc.

Online Monitoring of Anode Outlet CO Concentration in PEM Fuel Cells

Jingxin Zhang* and Ravindra Datta,z**

Department of Chemical Engineering, Fuel Cell Center, Worcester Polytechnic Institute, Worcester, Massachusetts 01609 USA

Anode gas outlet CO concentration is measured by an online infrared gas analyzer for a proton exchange membrane (PEM) fuel cell fed with H_2/100 ppm CO and with Pt or PtRu as anode catalyst. CO concentration increased with anode inlet flow rate at a given current density for Pt catalyst. CO outlet concentration with PtRu catalyst depended upon the current density at a cell temperature of 80°C. The CO concentration decreased with the increase of anode inlet flow rate at low current densities, while at higher current densities the outlet CO concentration followed a trend similar to that observed with Pt. The CO electro-oxidation rate on Pt and PtRu is thus calculated using CO material balance on the anode side. Results indicate that the enhanced tolerance of PtRu catalyst is due to the dual mechanisms of reduced CO affinity (ligand effect) and enhanced CO electro-oxidation rates (bifunctional effect), with either mechanism dominating depending on anode overpotential.
 [DOI: 10.1149/1.1523690]

Manuscript submitted June 20, 2002; revised manuscript received September 11, 2002. Available electronically October 31, 2002.

Reformed gas produced from conventional fuels such as gasoline, methanol, or natural gas are likely to be used in electric vehicle or stationary applications of proton exchange membrane (PEM) fuel cells. Regardless of the reforming processes employed, *e.g.*, steam reforming (SR) or autothermal reforming (ATR), the reformate gas largely consists of H_2, N_2, CO_2, CO, and H_2O. The strong poisoning effect of CO in the reformate gas on Pt-based anode catalyst has long been known[1,2] and extensively addressed.[3-12] However, attention in these studies has focused almost exclusively on the voltage-current characteristics of the PEM fuel cell under different operating conditions with Pt or Pt-based alloy catalysts and with a simulated reformate as anode feed.

We have reported a significant effect of the anode flow rate on PEM fuel cell performance with H_2/108 ppm CO feed and Pt as anode catalyst.[11] The results were explained on the basis of a CO inventory model which simulates the effect of flow rate on the anode overpotential via CO material balance in the anode chamber including terms for flow in and flow out, as well as electrocatalytic oxidation. The model predicts that the anode CO concentration is a function of anode flow rate, which had not been previously reported.

The present work was motivated by our desire to confirm the earlier model predictions[11] by direct on-line measurement of the CO concentration in PEM fuel cell anode outlet gas. In this paper, we provide such results based on using an infrared (IR) analyzer to monitor the anode outlet CO concentration of PEM fuel cell. Results are provided using both Pt and PtRu as anode catalyst at conventional PEM fuel cell operating conditions. The experimental data on the anode CO concentration as a function of anode flow rate for Pt catalyst agrees well with our previous predictions. Based on the CO material balance in the anode, the CO electro-oxidation rate is calculated for both Pt and PtRu catalyst. These results provide the first direct experimental evidence from *in situ* fuel cell experiments that both the ''bifunctional electro-oxidation mechanism'' and the ''ligand effect'' resulting in reduced CO affinity for the surface proposed in the literature coexist for PtRu catalyst.

Experimental

The complete experimental details are provided in our previous work;[11] a summary is given here. Gas diffusion electrodes loaded with 20 wt % Pt/C or PtRu/C, at a metal loading of 0.4 and 0.35 mg/cm^2, respectively, were purchased from E-TEK. Nafion® 115 PEMs (DuPont, Fayetteville, PA) were used after treatment. The membrane electrode assembly (MEA) was prepared by hot-pressing in a model C Carver hot press at 130°C under a pressure of 4000 lb for ~2 min. The MEA was then incorporated into a 5 cm^2 single cell from ElectroChem, Inc. (Woburn, MA), and tested in a test station with temperature, pressure, humidity, and flow rate control. The current-voltage characteristics were recorded using an HP 6060B dc electronic load, interfaced with a PC using LabView software (National Instruments, Austin, TX).

Anode and cathode gases were humidified in stainless steel bottles containing water at the desired temperature before being fed into the fuel cell. The total pressure of both anode and cathode was maintained at 30 psig. The volumetric flow rates reported in this study are all at the standard state (1 atm and 25°C) in units of standard cubic centimeters per minute (sccm). Premixed H_2/100 ppm CO was purchased from MG Industries (Morrisville, PA) and used as anode feed. The anode exit gas stream after the back pressure regulator first passes through a stainless steel filter (model 85, Parker Hannifin, Tewksbury, MA), to eliminate any particulates and water droplets. The gas stream then passes through a membrane gas dryer (MD series, Perma Pure Inc., Toms River, NJ) which further lowers the dew point of the gas stream to below 2°C before admission to the gas analyzer. A model 200 IR gas analyzer (California Analytical Instruments, Orange, CA) was used after calibration to monitor the exit CO concentration.

Results and Discussion

Our experiments show that the IR gas analyzer is suitable for online monitoring of CO concentration in the fuel cell anode outlet gas, especially in the 0-100 ppm range, which may be outside the accurate detection limit of gas chromatography.

Anode outlet CO concentration transient.—A typical CO outlet concentration response following the switching between a H_2 and a H_2/100 ppm CO feed is shown in Fig. 1. The corresponding cell voltage response at a constant current density of 200 mA/cm^2 and fuel cell temperature of 80°C is also shown. The anode inlet flow rate was constant at 48.1 sccm. Note that the cell voltage responds to CO introduction in the feed more quickly than the anode outlet CO concentration does. There is no significant CO concentration increase in the outlet during the initial rapid decrease of the cell voltage. The outlet CO concentration begins to increase only after there has been a significant decrease in the cell voltage. After this slow initial increase, the CO concentration rapidly rises and finally stabilizes at ~60 ppm, which is 40 ppm lower than the inlet CO concentration, despite the fact that the outlet H_2 flow rate is lower than the inlet H_2 flow rate by 7.6 sccm due to consumption of H_2 in the production of the current. These results indicate that there is an initial CO accumulation on the anode catalyst surface and in the anode chamber and tubing, such that the significant increase of out-

* Electrochemical Society Student Member.
** Electrochemical Society Active Member.
z E-mail: rdatta@wpi.edu

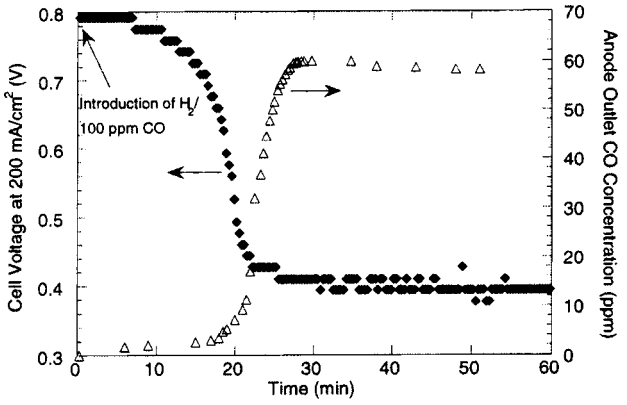

Figure 1. The transient of cell voltage and anode outlet CO concentration when the anode feed is switched from H_2 to H_2/100 ppm CO.

let CO concentration lags the decrease of the cell voltage by ~10 min. The overpotential under steady state conditions is ~0.4 V. Another conclusion evident from these results is that at steady state there is a finite rate of CO electro-oxidation even on Pt at practical operating conditions. This lends credence to our earlier explanation of the anode flow rate effect,[11] and also to other researchers' expectations on possible CO electro-oxidation on Pt in the PEM fuel cell anode.[4,8] Such real-time monitoring of the anode outlet CO concentration is planned to be used to determine *in situ* anode adsorption and kinetics in future work.

Anode outlet CO concentration at different flow rates for Pt catalyst.—Experiments were conducted at different anode inlet flow rates and at a constant current density as previously described,[11] with the results shown in Fig. 2. The fuel cell was operated at 80°C and a constant current density of 200 mA/cm^2 with Pt anode catalyst. The anode outlet CO concentration was determined to be a function of the anode inlet flow rate, as predicted.[11] The CO concentration increases from ~20 to 60 ppm when the anode inlet flow rate increased from 14 to 60 sccm. The data also follows the model predictions reasonably well. A quantitative explanation of this phenomenon can be found in Ref. 11. Qualitatively, the results may be explained as follows. When anode feed bearing CO is introduced, CO builds on the catalyst surface. During this process, the increase in CO concentration in anode chamber and outlet is small (Fig. 1). To sustain the given current density, the anode potential is polarized

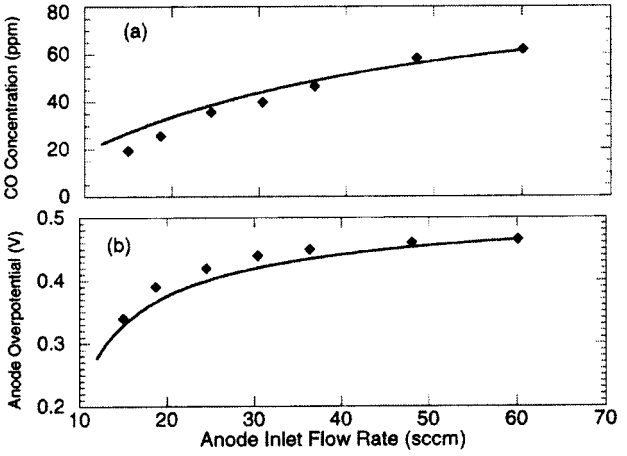

Figure 2. (a) Anode outlet CO concentration as a function of anode inlet flow rate. (b) Anode overpotential as a function of anode inlet flow rate. (♦) experimental data; (——) prediction based on previous model.[11] The fitting parameters used were $\alpha_{co} = 0.34$, $k_{oc} = 2.9 \times 10^{-7}$ A/cm^2, $\beta = 0.03$.

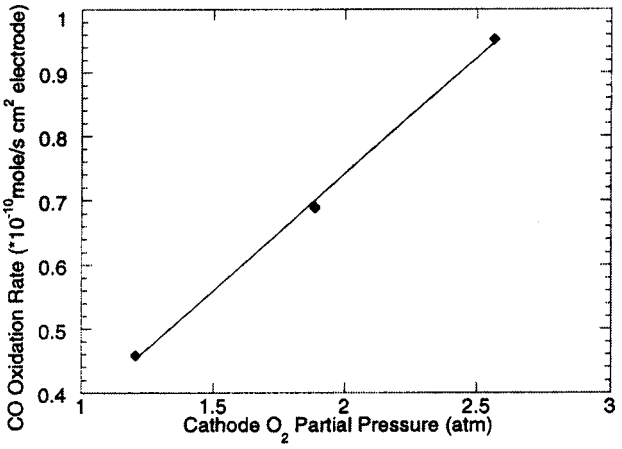

Figure 3. CO oxidation rate *vs.* cathode O_2 partial pressure in the nonelectrochemical reation.

to higher values, which also promotes the electro-oxidation of CO. Eventually, a steady state is reached for both overpotential and CO concentration, reflecting a balance between the rate of CO in and the rate of CO out plus the rate of its electro-oxidation. Were there no electro-oxidation, the CO outlet concentration would be higher than the inlet concentration, because some H_2 is consumed. An increase of the anode inlet flow rate introduces more CO into the anode chamber, which increases the anode CO concentration and, consequently, the CO surface coverage of Pt catalyst. Thus, the anode potential is polarized to an even higher value, which further accelerates the CO oxidation rate. Therefore, a new steady state with new values of anode overpotential and anode CO concentration is reached (Fig. 7 and 10 in Ref. 11).

CO oxidation by O_2 permeating through the proton exchange membrane.—We have reported that O_2 permeating through the membrane from the cathode contributes to the CO clean up in the anode chamber.[11] To determine the amount of CO thus oxidized via the nonelectrochemical oxidation, experiments were conducted with the fuel cell simply as a catalytic membrane reactor, *i.e.*, with all the electronic connections between the cathode and anode disconnected, *e.g.*, the electronic load or the multimeter used to monitor the cell voltage. All other experimental conditions were identical to that employed in the fuel cell performance test. Thus, the fuel cell was acting as a membrane reactor, with O_2 diffusing through the PEM from the cathode and then reacting with CO and H_2 at the anode. The CO mass balance directly proves our previous hypothesis that CO is oxidized by permeating O_2. A typical result is shown in Fig. 3. In this experiment, the fuel cell temperature was set at 80°C and the anode inlet flow rate was 15 sccm, while the cathode total pressure was set at 30, 20, and 10 psi, respectively. The CO oxidation rate (normalized to the electrode geometric area) is plotted against the cathode O_2 partial pressure (the water vapor partial pressure is subtracted from the cathode total pressure, assuming that the cathode chamber is saturated by water vapor at 80°C). Figure 3 shows that there is a finite CO oxidation due to the nonelectrochemical catalytic reaction between CO and permeating O_2.

Note that the CO oxidation rate is linearly dependent on the cathode O_2 partial pressure. This can be justified by the model mentioned previously,[11] where it is assumed that cathode O_2 dissolves in the swollen Nafion membrane and then diffuses to the anode. It is further assumed that the oxidation of CO by permeating O_2 from the cathode is controlled by the rate of permeation of O_2 through the membrane.

CO electro-oxidation rate on Pt anode catalyst.—Because we have directly determined the contribution of CO oxidation in the

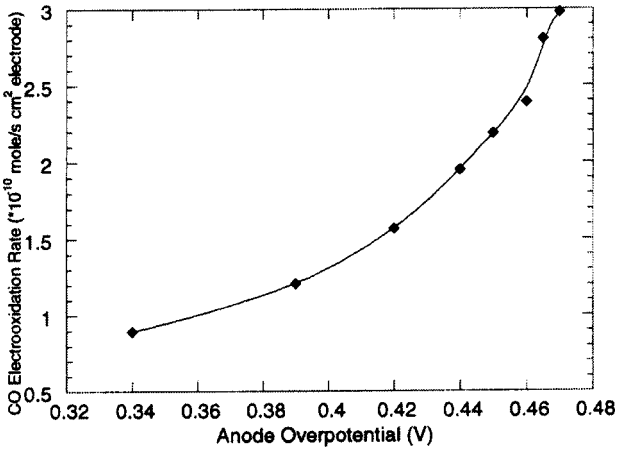

Figure 4. CO electro-oxidation rate as a function of anode overpotential.

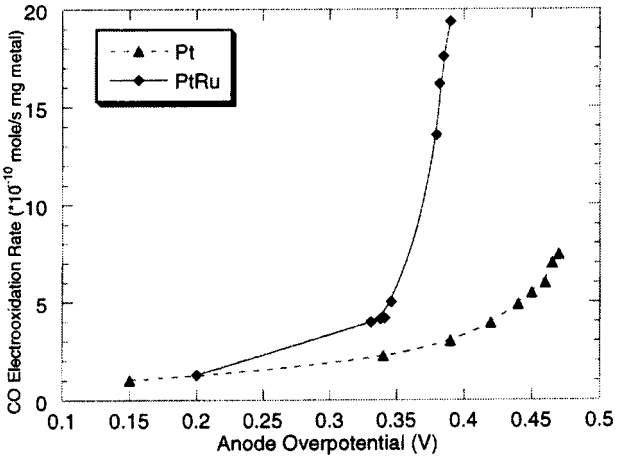

Figure 6. Comparison of CO electro-oxidation rate on Pt and PtRu anode catalyst at 80°C. Anode inlet flow rates varied between 15 and 84 sccm.

nonelectrochemical reaction by the permeating O_2, the CO electro-oxidation rate can be calculated based on CO material balance, subtracting the rate of the nonelectrochemical oxidation. The results are shown in Fig. 4, in which the calculated CO electro-oxidation rate normalized to the electrode geometric area is plotted as a function of anode overpotential, determined as described in Ref. 11. The CO electro-oxidation rate is calculated at different anode flow rates, which vary from 14 to ~60 sccm. It is shown that the electro-oxidation rate is on the order of 10^{-10} mol/s cm^2 electrode at the fuel cell operation conditions used in this study. The electro-oxidation rate increases with the anode overpotential exponentially, as expected per the Butler-Volmer equation. This is, to our knowledge, the first *in situ* experimental evaluation of CO electro-oxidation rate on Pt catalyst in an operating PEM fuel cell.

Anode outlet CO concentration at different flow rates for PtRu catalyst.—To compare the response of different anode catalysts toward CO impurity in the feed stream, PtRu was also used as the anode catalyst. Figure 5 shows the anode outlet CO concentration of a PEM fuel cell at 80°C as a function of anode flow rate for various constant current densities ranging from 200 to 700 mA/cm^2. The feed stream contains 100 ppm CO, as indicated by the horizontal line in the center of the figure. At current density larger than 500 mA/cm^2, a trend similar to that with Pt anode catalyst is observed, *i.e.*, the anode CO concentration is below the feed concentration and increases with the anode inlet flow rate. However, when the current density is below 400 mA/cm^2, the CO concentration profile shifts to the region above the feed CO concentration. This distinctly different behavior is especially apparent for low current densities, *e.g.*, 200 mA/cm^2, for which at a flow rate of about 16 sccm (corresponding to a stoichiometry of 2.1), the CO outlet concentration is nearly doubled. This means that at the current density of 200 mA/cm^2, there is no significant CO electro-oxidation occurring at the anode. Practically all the CO entering the anode leaves the anode. Because at low anode inlet flow rates a significant fraction of H_2 is consumed, the outlet CO becomes more concentrated than the feed. As the feed rate is increased, the outlet CO concentration declines asymptotically to the feed concentration at high flow rates, as a smaller fraction of H_2 feed is consumed. Thus the observed trend of the outlet CO concentration variation with the anode inlet flow rate for PtRu is opposite to that observed with Pt. A material balance indicates that at 200 mA/cm^2 the difference between CO entering and exiting the fuel cell anode is ~3%. It is thus clear that at the current density of 200 mA/cm^2 on PtRu anode catalyst, the CO electro-oxidation rate is negligible. This clearly indicates that the adsorption of CO on PtRu is weaker as compared with Pt, and thus this current density can be sustained without significantly higher overpotential.

The effect of anode inlet flow rate on anode overpotential is less appreciable for PtRu, as compared to Pt catalyst. For example, the anode overpotenial is about 0.2 V at 200 mA/cm^2, and about 0.38 V at 700 mA/cm^2 for anode inlet flow rates between 15 and 84 sccm.

Comparison of CO electro-oxidation rate on Pt and PtRu at 80°C.—To compare the CO electro-oxidation rate on Pt and PtRu catalyst, the CO electro-oxidation rate is further normalized to the catalyst loading and plotted *vs.* anode overpotential in Fig. 6. Note that contrary to the case of Pt catalyst, we did not observe experimentally that O_2 partial pressure has a significant effect on the anode overpotential at a given current density for PtRu catalyst at 80°C. Figure 6 shows that the CO electro-oxidation rate is small in lower overpotential range (*e.g.*, <0.3 V) for both Pt and PtRu catalyst, but increases dramatically in the anode overpotential range between 0.35 and 0.4 V for PtRu. The electro-oxidation rate does not "ignite" until after the overpotential range of 0.45-0.5 V for Pt catalyst, a difference of roughly 0.1 V between the two catalysts. This figure looks qualitatively similar to the cyclic votammetry (CV) curve of H_2/CO electro-oxidation on Pt and PtRu in liquid electrolyte, except the fact that the results in this work are obtained from steady state data in a functioning fuel cell. Moreover, the so-called ignition potential for CO oxidation is quite comparable to the CV results (see Fig. 7 of Ref. 3 and Fig. 7 of Ref. 13). Note that the CO electro-oxidation rate is on the order of 10^{-10} to 10^{-9} mol/s mg PtRu at 80°C in the potential range shown in this study. In CV

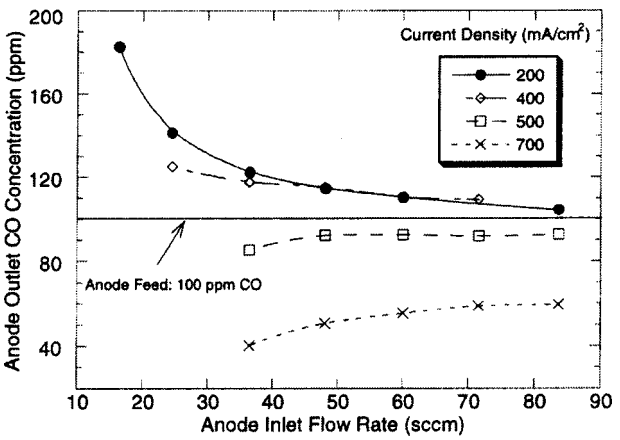

Figure 5. Anode outlet CO concentration as a function of anode inlet flow rate at various constant current densities.

studies, the kinetic information cannot be easily obtained, especially in the relatively high overpotential region, due to the diffusion limitation of the reactant gas in the liquid electrolyte. In addition, it is difficult to distinguish the CO electro-oxidation current from that of hydrogen when H_2/CO mixture is studied. Thus, the experiment in this study offers a convenient and simple way to obtain *in situ* kinetic information of CO electro-oxidation in a PEM fuel cell anode.

The results in this study also offer strong evidence for clarifying the CO tolerance mechanism of PtRu catalyst. A well-accepted mechanism is the ''bifunctional'' mechanism,[3,14] in which it is believed that oxygen-containing species, *e.g.*, OH, nucleate on Ru at lower electrode potentials than on Pt, so that CO is electro-oxidized from the catalyst surface, generating additional free surface sites for H_2 oxidation. On the other hand, a recent extended X-ray absorption fine structure (EXAFS) and adsorption study by Lin *et al.*[15] supports the ''ligand'' mechanism, *i.e.*, the interaction of CO with the alloyed PtRu catalyst is weakened as compared to Pt leading to lower surface coverage. Furthermore, the surface diffusion activation energy of CO on PtRu is also shown to decrease due to the Ru alloying effect, *i.e.*, by reducing the back donation of electrons from Pt, as demonstrated by an NMR study.[16] These results support the ''ligand'' mechanism,[12,17,18] *i.e.*, the introduction of a second element such as Ru modifies the electronic structure of Pt by removing electron density from Pt atoms, so that the Pt-CO bond is weakened and the equilibrium surface coverage of CO is reduced, making more free surface sites available for hydrogen electrooxidation.

The results here clearly indicate that in fact both of these mechanisms are responsible for the enhanced tolerance of PtRu catalyst. At relatively low overpotential (*e.g.*, <0.2 V), the ''ligand'' effect of reduced CO affinity dominates and PtRu catalyst is ''CO tolerant'' in a true sense at the lower current densities. This is supported by the fact that in this overpotential region the CO electro-oxidation rate on PtRu is very small and is roughly the same as Pt catalyst. The anode CO content is strongly dependent on the anode inlet flow rate, and anode CO concentration well above that of the inlet is observed (Fig. 5). At relatively high overpotentials (*e.g.*, >0.35 V), on the other hand, the ''bifunctional'' mechanism dominates. In this potential region, the CO electro-oxidation rate is well above that of Pt catalyst, with CO oxidation igniting about 100-150 mV earlier than that on Pt catalyst. A recent study by Lu *et al.*[19] using temperature-programmed desorption coupled with mass spectroscopy also proposes that both mechanisms coexist for the CO tolerance of PtRu catalyst. They give a quantitative estimation of the contribution of both mechanisms, but the effect of electrode potential cannot be explicitly evaluated in their nonelectrochemical experiments. Liu and Norskov[20] also show that both mechanisms contribute to the CO tolerance of PtRu through DFT calculations, though the authors seem to favor the ''ligand'' effect as the dominating mechanism for the CO tolerance of PtRu in PEM fuel cell.

It is thus seen that the monitoring of anode outlet CO concentration is useful in understanding the CO tolerance mechanism for different anode catalytic materials and in their direct evaluation and comparison. It is conceivable that the online monitoring of the outlet CO concentration may provide additional insights into the mechanism of CO poisoning as well as CO_2 poisoning of other alloy catalysts. Such studies are in progress.

Conclusions

We have shown that the direct online monitoring of the PEM fuel cell anode outlet CO concentration using an IR gas analyzer provides important insights into the mechanism of CO electro-oxidation. The anode CO concentration is a function of anode flow rate at a constant current density. The CO concentration increase with anode inlet flow rate when Pt is used as anode catalyst agrees reasonably well with our previous model predictions.[11] The CO outlet concentration behavior with PtRu catalyst is especially interesting and depends upon the current density at a cell temperature of 80°C. The anode CO concentration decreased with the increase of anode inlet flow rate at low current densities, while at higher current densities, the outlet CO concentration follows the same trend as that observed for Pt anode catalyst. The CO electro-oxidation rate is calculated using CO material balance in the anode and compared as a function of anode overpotential for Pt and PtRu catalyst. The results indicate that the enhanced tolerance of PtRu catalyst is due to the dual action of reduced CO affinity (ligand effect) and enhanced electro-oxidation rates (bifunctional effect).

Acknowledgment

The authors thank Dr. Sean Emerson of HydrogenSource for suggestions on the filter and water drying setup for the gas stream before gas analyzer. J.Z. also gratefully acknowledges the Dr. Chuesan Yoo Fellowship for partial support of his graduate study.

Worcester Polytechnic Institute assisted in meeting the publication costs of this article.

References

1. W. Vogel, J. Lundquist, P. Ross, and P. Stonehart, *Electrochim. Acta*, **20**, 79 (1975).
2. S. Gottesfeld and J. Pafford, *J. Electrochem. Soc.*, **135**, 2651 (1988).
3. H. A. Gasteiger, N. M. Markovic, and P. N. Ross, *J. Phys. Chem.*, **99**, 16757 (1995).
4. R. J. Bellows, E. P. Marucchi-Soos, and D. T. Buckley, *Ind. Eng. Chem. Res.*, **35**, 1235 (1996).
5. H.-F. Oetjen, V. M. Schmidt, U. Stimming, and F. Trila, *J. Electrochem. Soc.*, **143**, 3838 (1996).
6. R. J. Bellows, E. Marucchi-soos, and R. P. Reynolds, *Electrochem. Solid-State Lett.*, **1**, 69 (1998).
7. S. J. Lee, S. Mukerjee, E. A. Ticianelli, and J. McBreen, *Electrochim. Acta*, **44**, 3283 (1999).
8. T. E. Springer, T. Rockward, T. A. Zawodzinski, and S. Gottesfeld, *J. Electrochem. Soc.*, **148**, A11 (2001).
9. Z. Qi, C. He, and A. Kaufman, *Electrochem. Solid-State Lett.*, **4**, A204 (2001).
10. M. Murthy, M. Esayian, A. Hobson, S. MacKenzie, W. Lee, and J. W. Van Zee, *J. Electrochem. Soc.*, **148**, A1141 (2001).
11. J. Zhang, T. Thampan, and R. Datta, *J. Electrochem. Soc.*, **149**, A765 (2002).
12. S. Ball, A. Hodgkinson, G. Hoogers, S. Maniguet, D. Thompsett, and B. Wong, *Electrochem. Solid-State Lett.*, **5**, A31 (2002).
13. T. J. Schmidt, H. A. Gasteiger, and R. J. Behm, *J. Electrochem. Soc.*, **146**, 1296 (1999).
14. M. Watanabe and S. Motoo, *J. Electroanal. Chem.*, **60**, 275 (1975).
15. S. Lin, T. Hsiao, J. Chang, and A. Lin, *J. Phys. Chem. B*, **103**, 97 (1999).
16. Y. Tong, H. Kim, P. K. Babu, P. Waszczuk, A. Wiechowski, and E. Oldfield, *J. Am. Chem. Soc.*, **124**, 468 (2002).
17. P. C. Mitchell, P. Wolohan, D. Thompsett, and S. Cooper, *J. Mol. Catal. A: Chem.*, **119**, 223 (1997).
18. M. Krausa and W. Veilstich, *J. Electroanal. Chem.*, **379**, 307 (1994).
19. C. Lu and R. Masel, *J. Phys. Chem. B*, **105**, 9793 (2001).
20. P. Liu and J. K. Norskov, *Fuel Cells*, **1**, 192 (2001).